Journal of Molecular Structure 1352 (2026) 144424

Contents lists available at ScienceDirect

Journal of Molecular Structure

journal homepage: www.elsevier.com/locate/molstr

Ethyl 4-methyl-2-(phenylamino)thiophene-3-carboxylate: One-pot synthesis, structural characterization, computational studies, and antitumor activity

Abdullatif Bin Muhsinah [a], Nabila A. Kheder [b], Saied M. Soliman [c], Ismail A. Elhaty [d,*], Yahia N. Mabkhot [e,*]

[a] Department of Pharmacognosy, College of Pharmacy, King Khalid University, P.O. Box 960, Abha 61421, Saudi Arabia
[b] Department of Chemistry, Faculty of Science, Cairo University, Giza 12613, Egypt
[c] Department of Chemistry, Faculty of Science, Alexandria University, Ibrahimia, Alexandria, Egypt
[d] Department of Nutrition and Dietetics, Faculty of Health Sciences, Istanbul Gelisim University, Istanbul, Turkey
[e] Department of Pharmaceutical Chemistry, College of Pharmacy, King Khalid University, Abha 61441, Saudi Arabia

ARTICLE INFO

Keywords:
Thiophene
Chemoselective reaction
Hirshfeld surface analysis
Fukui function
Anticancer activity

ABSTRACT

Ethyl 4-methyl-2-(phenylamino)thiophene-3-carboxylate (**8**) was synthesized via a one-pot three-component reaction of ethyl 3-oxobutanoate, PhNCS, and 1-chloropropan-2-one in NaOEt. This process offers several advantages over previously reported synthetic method, including high yield, less reaction time and availability of the starting materials. Spectral data and X-ray analysis were used to elucidate the structure. Its structure is stabilized by a strong intramolecular N—H…O hydrogen bond. Hirshfeld analysis indicated the most dominant non-covalent interactions are C…H (26.3 %) and H…H (53.9 %), where the C11…H2 (2.760 Å) and C7…C7 (3.314 Å) contacts are the shortest contacts. In addition, DFT-based computational studies were performed to assess the electronic structure and local reactivity of thiophene **8**. HOMO–LUMO energy gaps, MEP surface mapping, Mulliken charge distribution, and Fukui function analyses were used to identify the key electrophilic and nucleophilic centers within the molecules. Antitumor activity of thiophene **8** was assessed against HepG2 (liver cancer), MCF-7 (breast cancer), and HCT116 (colorectal cancer) by means of the sulforhodamine B (SRB) assay. The compound exhibited promising anticancer activity, showing its highest potency against HepG2 (IC_{50} =40.1 ± 1.3 μg/mL) compared to MCF-7 (76.3 ± 2.5) and HCT-116 (92.9 ± 2.02 μg/mL) cell lines.

1. Introduction

Cancer poses a great threat to the life and wellbeing of many across the world. It is the second most common cause of mortality globally [1, 2]. Additionally, it causes several morbidities that affect patients' quality of life and forms a burden on countries' healthcare resources [3]. Among the most challenging aspects in cancer treatment are the cytotoxic effects of its drugs to normal cells, in addition to drug' resistance, which decreases their efficacy [4,5]. These problems can be addressed by preparing new, more selective antiproliferative agents.

Thiophene-containing compounds were reported to have numerous pharmacological properties, including anticancer [1–5], antimicrobial [6], antioxidant [7], antithrombotic [8], analgesic, and anti-inflammatory [9]. Also, many marketed medications contain a thiophene core, such as antimigraine pizotifen, antihistamine ketotifen, antiplatelet ticlopidine, antifungal tioconazole, psychostimulant benocyclidine, and local anesthetic articaine (Fig. 1). Also, thiophene derivatives have been reported to bind with a wide range of cancer-specific protein targets. Moreover, thiophene derivatives (modified chalcones) showed selective sensing of metal ions in the solution [10]. The kind and location of substitutions in the thiophene moiety have been shown to affect their binding ability [15].

The reaction of active methylene reagents with PhNCS and α-halo compounds in a basic medium led to the synthesis of thiophene [11,12], or 1,3-thiazole derivatives [13–18]. Changing either the substituents attached to the active methylene group or the basic catalysts can lead to the synthesis of either thiophene or thiazole derivatives.

Inspired by the above mentioned results and in continuation of our

* Corresponding authors.
E-mail addresses: iaeismail@gelisim.edu.tr (I.A. Elhaty), alzooba8@gmail.com (Y.N. Mabkhot).

https://doi.org/10.1016/j.molstruc.2025.144424
Received 15 August 2025; Received in revised form 4 October 2025; Accepted 16 October 2025
Available online 17 October 2025

research studies on development of new and cost-effective synthetic methods to prepare a variety of heterocycles with promising pharmacological activities [4,19–21], herein, we present an efficient synthetic procedure to obtain title compound using easily accessible substrates, in addition to studying its 3D structure using X-ray analysis. The Supramolecular structure of **8** is described using Hirshfeld topology calculations. The antitumor activity of **8** against HepG2, MCF-7, and HCT116 cell lines is also presented.

2. Materials and methods

2.1. General remarks

All reagents and solvents were bought from usual commercial sources, including (Aldrich, purity >99 %, St. Louis, MO, USA), and used without further purification. In open glass capillaries, all the melting points were determined using a Gallen Kamp apparatus (Thermofisher Scientific, Paisley, UK) and were uncorrected. Infrared (IR) spectra were measured using the potassium bromide disk technique on Perkin Elmer FT-IR 1000 (PerkinElmer, Waltham, MA, USA). A Bruker advanced NMR spectrometer running at 400 MHz in deuterated DMSO was used to measure the NMR spectra. Elemental composition was analyzed using a Vario Elemental Analyzer III (Vario, Germany). Using the sulforhodamine B assay, anticancer properties of synthesized compound were assessed against three types of human cancer cell lines namely MCF-7, HepG2, and HCT-116.

2.2. *Synthesis of ethyl 4-methyl-2-(phenylamino)thiophene-3-carboxylate (8)*

A solution of ethyl 3-oxobutanoate (**1**) (1.30 g, 10 mmol) in NaOEt [Na (0.23 g) in absolute EtOH (20 ml)] was stirred for 30 min. Then, PhNCS (1.35 g, 10 mmol) was added, and stirring continued for 1 hour. 1-Chloropropan-2-one (0.92 g, 0.01 mol) was added to the reaction mixture, and stirring was continued for three more hours. The reaction mixture was poured into an ice/water mixture, and neutralized using dil. HCl. The solid product was filtered off, washed with H_2O, and dried. Recrystallization from ethanol afforded thiophene derivative **8**, in 75% yield; m.p. 55-6 °C [Lit. mp. 55-58 °C [22]; IR (KBr) ν_{max}: 3175 (NH), 3098 (CH aromatic), 2959 (CH aliphatic), 1655 (C=O) cm^{-1}; MS (ESI-QTOF): calcd. for $[M+H]^+$ $m/z = 262.09$; found 262.0807; ^{1}H NMR (400 MHz, DMSO-d_6) δ 1.31 (t, 3H, CH_3, $J = 7.08$ Hz), 2.28 (s, 3H, CH_3), 4.27 (q, 2H, CH_3, $J = 7.08$ Hz), 6.28 (s,1H, CH), 7.07 (t, 1H, $J = 7.2$ Hz, ArH), 7.31-7.40 (m, 4H, ArH`s), 9.97 (s,1H, NH); ^{13}C NMR (100 MHz, DMSO-d_6) δ 14.60, 18.52, 60.20, 105.21, 107.88, 118.90, 123.35, 130.00, 135.95, 141.25, 159.37, 166.01. Anal Calcd. For $C_{14}H_{15}NO_2S$ (261.34): C, 64.34; H, 5.79; N, 5.36. Found. C, 64.42; H, 5.88; N, 5.28.

2.3. *X-ray crystallography*

Thiophene **8** was obtained as single crystals by slow evaporation from an ethanol solution of the pure compound at room temperature. Data were collected on a Bruker APEX-II D8 Venture area diffractometer, equipped with graphite monochromatic Mo Kα radiation, λ = 0.71073 Å at 293 (2) K. Cell refinement and data reduction were carried out by Bruker SAINT. SHELXT [23,24] was used to solve the structure. The final refinement was carried out by full-matrix least-squares techniques with anisotropic thermal data for nonhydrogen atoms on *F*. CCDC 2449718 contains the supplementary crystallographic data for this compound, which can be obtained free of charge from the Cambridge Crystallographic Data Centre via www.ccdc.cam.ac.uk/data_request/cif.

2.4. Computational studies

Hirshfeld surface analysis is performed using the Crystal Explorer 17.5 software [25]. In addition, the molecular structure of the obtained

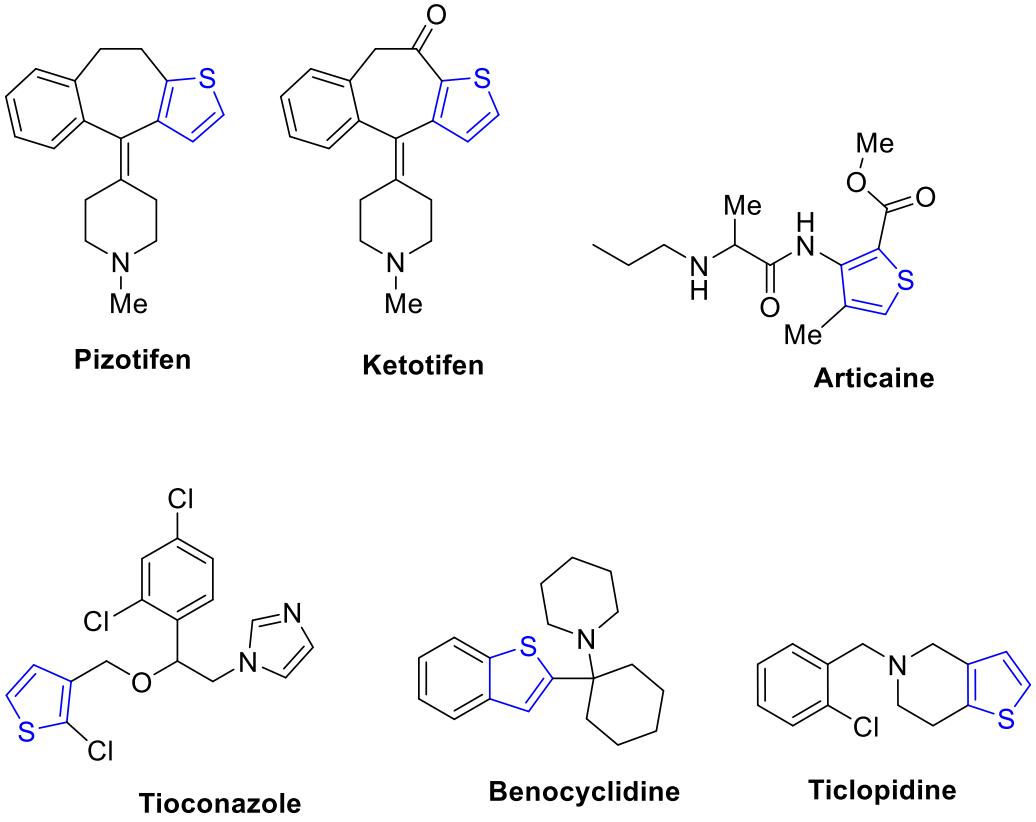

Fig. 1. Medications contain a thiophene core.

thiophene **8**, was depicted using ChemDraw 16.0 [26]. To study its molecular behavior, this molecule was subjected to optimization and energy minimization under default conditions utilizing the density functional theory (DFT), B3LYP method and the 6–311++*G*(d,p) basis set. Gaussian 09 W software was used for DFT calculations [27], and the obtained results were interpreted using GaussView 6.0. A 13th Gen Intel® Core™ i7–1360Pm 2.20 GHz CPU and 16.0 GB RAM laptop was used in all calculations.

Frontier molecular orbitals (FMO) analysis was conducted to assess the chemical reactivity and stability of the title compound. The highest occupied and lowest unoccupied molecular orbitals (HOMO and LUMO, respectively), and the band gap (ΔE) energies were computed using the forementioned DFT method and Gaussian 09 W software. ΔE value is a good indicator of the molecule's chemical stability and reactivity. A larger energy gap typically correlates with enhanced stability and reduced chemical reactivity.

Fukui function was used to study the local reactivity of all atoms in thiophene **8** to identify the nucleophilic and electrophilic attack sites using Gaussian 09 W and visualized on GaussView 6.0. Thiophene **8** was optimized under neutral conditions using DFT, B3LYP method, and the 6–311++*G*(d,p) basis set [28]. In addition, natural bond orbital (NBO) analysis was performed using the NBO program implemented in Gaussian 09 W by applying the POP=NBO keyword [29]. Fukui function and other parameters were studied using the UCA-FUKUI computational tool [30].

The molecular electrostatic potential (MEP) surface was employed to study the 3D charge distribution across the molecule. It indicates the molecules' reactivity towards electrophiles or nucleophiles using the DFT method, B3LYP, and the 6–311++*G*(d,p) basis sets. The MEP map displays the reactive sites of a molecule in different colors, where the most electron-rich (negative) sites carry the red color, and electron-deficient (positive) sites are blue colored. It helps understand the intermolecular interactions, such as oxygen and nitrogen atoms as hydrogen bond acceptors [31].

For further investigation of the charge distribution across compound **8**, Mulliken atomic charge analysis was conducted using the DFT method and the aforementioned level of theory. Molecular characteristics are affected by the molecule's atomic charge distribution, such as intermolecular and intramolecular bonding, system's dipole moment, polarization, and electronic structure.

The reactivity and stability of thiophene **8** were further studied using electronegativity (χ), chemical potential (μ), global hardness (η), global softness (S), and the electrophilicity index (ω), based on conceptual DFT and HOMO and LUMO energies.

2.5. The in vitro antitumor assessment

Liver carcinoma cells (HepG2), Human breast adenocarcinoma (MCF-7), and colon adenocarcinoma (HCT 116) cell lines were provided by the American Type Culture Collection (ATCC, Boston, MA, USA). RPMI 1640 medium, supplemented with 10 % foetal bovine serum and 100 IU/mL PS (penicillin/streptomycin), was used to culture HepG2, MCF-7, and HCT 116 cell lines

The sulforhodamine B (SRB) assay was used to assess the anticancer efficacy of compound **8**. HepG2, MCF-7, and HCT 116 cell lines were plated in 96-well plates at a density of 2×10^3 cells per well. The cells were left to adhere for a full day before being treated with nanoemulsion applications. Various concentrations of the formulations (0, 0.01, 0.1, 1, 10, 100, and 1000 μg/mL) were applied to the wells, and the cells were incubated for 72 h at 37 °C. After this incubation period, the culture media was replaced with 150 μL of 10 % trichloroacetic acid and incubated for 1 h. at 4 °C, followed by five washes with distilled H_2O. The cells were then stained with 50 μL of a 0.04 % w/v SRB solution and incubated for 10 min. at 25 °C in the dark. Afterward, the excess stain was removed with 1 % CH_3COOH, and 100 μL of 10 mM Tris base solution (pH=10.5) was added to each well to dissolve the protein-bound dye. The optical density was measured using a microplate reader set to 540 nm [32].

2.6. Drug likeness and molecular property prediction

The *in silico* evaluation of thiophene **8** was performed using the OSIRIS Property Explorer tool [33]. The molecular structure was analyzed to obtain key physicochemical parameters, including calculated log P (cLogP), aqueous solubility (log S), molecular weight, and topological polar surface area (TPSA). OSIRIS was also used to predict the potential toxicity risks such as mutagenicity, tumorigenicity, irritant effects, and reproductive toxicity. The drug-likeness and drug-score values were generated to assess the compound's suitability as a drug candidate.

3. Results and discussion

3.1. Synthesis and characterization

Schäfer *et al.* reported the synthesis of thiophene **8** [22] *via* the reaction of ethyl 2-amino-4-methylthiophene-3-carboxylate (**11**) [34] with aniline. Herein, a modified one-pot method was developed for the synthesis of **8** using easily accessible reagents as outlined in Scheme 1. Initially, ethyl 3-oxobutanoate (**1**) in sodium ethoxide was stirred at room temperature for 30 min, then PhNCS was added to give sodium salt **3**. Then, treatment of **3** with 1-chloropropan-2-one (**4**) gave **5**.

Heterocyclization of **5** can lead to the formation of thiophene **7** or thiazole **10**. Spectral data of the isolated product confirmed the thiophene structure **8**, obtained *via* the deacetylation reaction of **7** under experimental conditions. This result is in complete agreement with previous studies [35,36]. For example, in the NMR spectra of the isolated product [**Figs. S2** and **S3**], the absence of protons and carbon signals due to acetyl function allowed us to exclude structures **7** and **10**. The thiophene structure **8** was also evidenced using proton NMR spectral data, which revealed the presence of methyl, ethoxy, thiophene, NH, and phenyl protons, as expected for this chemical skeleton (**SI file**).

3.2. X-ray structure description

The X-ray structure analysis of this compound confirmed the formula $C_{14}H_{15}NO_2S$, which is in accord with other characterizations. Its crystal system is monoclinic, and the space group is $P2_1/n$. The unit cell parameters *a, b, c*, and β are 9.8042(4), 5.7212(2), 23.6360(9), and 90.954 (4) °, respectively, while $z = 4$ and unit cell volume of 1325.60(9) Å^3 (**Table S1**). The molecular structure is stabilized by a strong intramolecular N1-H7…O2 hydrogen bond where the H7…O and N1…O2 distances are 1.99 and 2.684(3) Å, respectively (Fig. 2). A view of packing is shown in the same figure along the crystallographic *b*-direction.

Table 1 shows that the results obtained by DFT optimization of compound 8 are in accordance with X-ray values, with bond lengths typically within 0.03 Å and angles within about 1° of the X-ray values. This suggests that the chosen level of theory provides a reliable computational model for interpreting reactivity and noncovalent interactions discussed in this manuscript [37].

3.3. Hirshfeld surface analysis

Intermolecular interactions play an important role in the packing of molecules in the solid-state crystalline materials. Each crystal has its unique packing features, which cooperate to stabilize the crystalline structure, holding the molecules in a specific arrangement. This tool is significant for studying the molecular topology, intermolecular interactions within the crystal structure of targeted molecule, and the effect of the closed molecular contacts on these interactions. Hence, the analysis of intermolecular contacts using Hirshfeld analysis gave strong

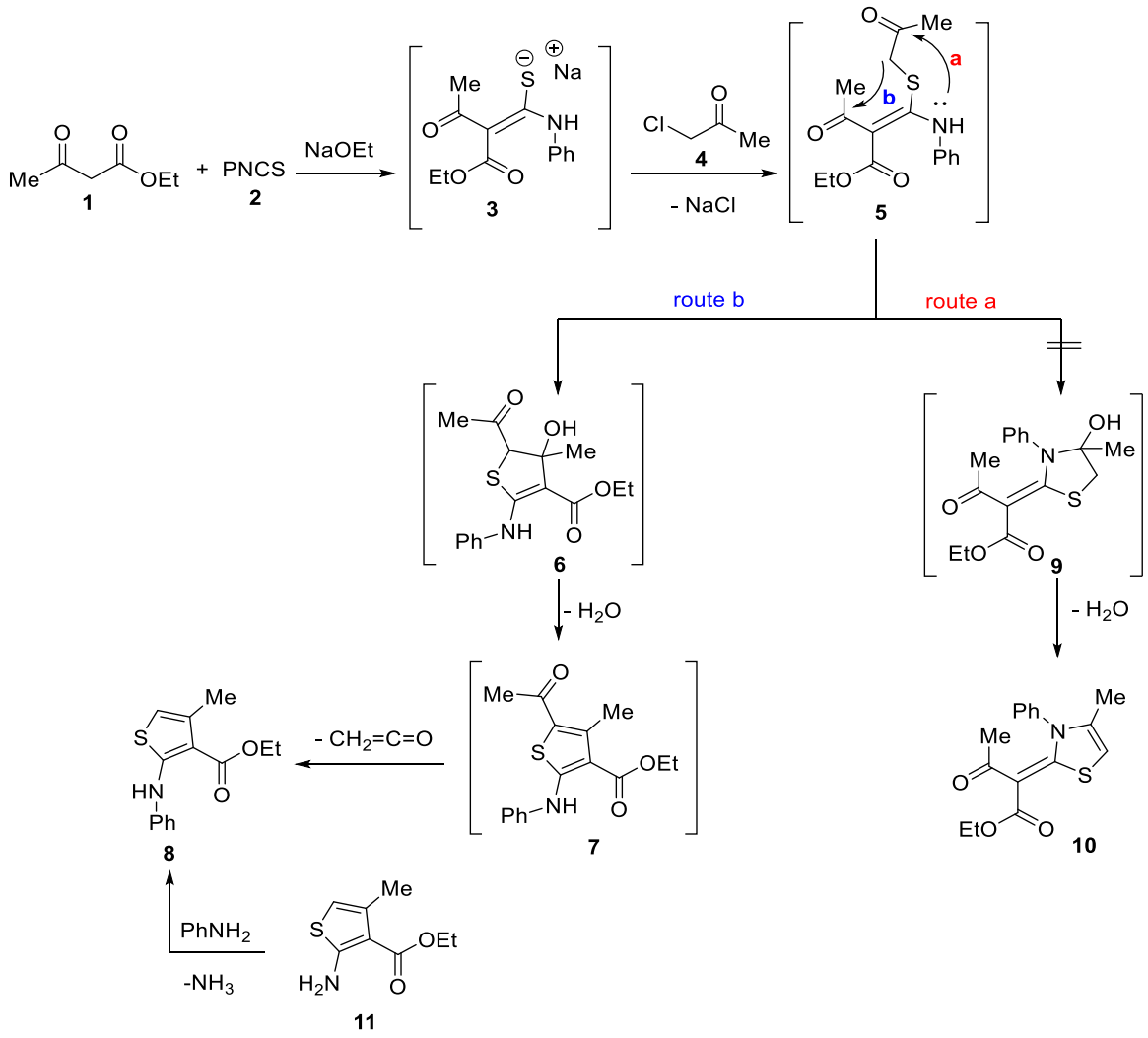

Scheme 1. Preparation of thiophene derivative **8**.

insights into the molecular packing. There are many short and long distance contacts contributing to different extents in the molecular packing of **8**. These contacts are H…H, C…H, C…C, N…H, O…H, C…O, S…H, S…C, S…N and S…O. Among these contacts, the most abundant contacts are the C…H (26.3 %) and H…H (53.9 %). The C11…H2 (2.760 Å) and C7…C7 (3.314 Å) contacts appeared as red spots in the d_{norm} map and are considered the most significant for molecular packing (Fig. 3). No evidences for the d_{norm}, shape index, and curvedness maps about the presence of any significant π-π stacking interactions.

3.4. Fukui functions

The optimized structure of thiophene **8** is shown in Fig. 4. The Fukui function is a significant computational tool used to investigate the change in the electron density of a molecule after adding and removing electrons, so it can indicate the molecule's chemical reactivity and site selectivity using density functional theory (DFT) [38]. This approach determines the most susceptible sites in the molecule to electrophilic, nucleophilic, and radical attack. The following approximations are used to express the Fukui function [39],

Electrophilic reactions: $f_k^- = q_k\,(N_0) - q_k\,(N_0 - 1)$

Nucleophilic reactions: $f_k^+ = q_k\,(N_0 + 1) - q_k\,(N_0)$

Radical reactions: $f_k^0 = \frac{1}{2}\left(f_k^+ + f_k^-\right)$ where q_k, (N_0), $(N_0 + 1)$, and $(N_0 - 1)$ represent the electronic population of atom k, the molecule in its neutral state, the molecule in its anionic state, and the molecule in its cationic state, respectively.

Dual Descriptor index $(\Delta f(r))$ is also used to predict the reactivity of atomic sites and selectivity towards nucleophilic or electrophilic attack. Dual Descriptor is the difference between f_k^+ and f_k^-, calculated as follows $\Delta f(r) = [f^+(r) - f^-(r)]$. If $\Delta f(r) > 0$, the site prefers a nucleophilic attack, while if $\Delta f(r) < 0$, it prefers an electrophilic attack.

f_k^-, f_k^+, f_k^0, and $\Delta f(r)$ values are represented in **Table S2**. The obtained results show that **H28, C1, S5**, and **C13** possess high values of f_k^+ and positive values of $\Delta f(r)$ make these atoms the most susceptible sites for the nucleophilic attack. On the other hand, atoms **N6, C4, C2**, and **C10** show high f_k^- values and negative $\Delta f(r)$ values make these atoms the most favorable sites for electrophilic attack. The obtained findings reveal diverse reactive behavior across the molecule. For example, heteroatoms like **N6** exhibit significant susceptibility to electrophilic attack, primarily due to their electron-dense character. Moreover, the aromatic thiophene ring contributes nucleophilic properties to the compound, which can be influenced by the presence or position of substituents.

3.5. Molecular electrostatic potential (MEP)

The molecular electrostatic potential (MEP) map of optimized thiophene **8** was generated using the B3LYP/6–311++*G*(d,p) method providing a detailed visualization of the molecule's electrostatic potential distribution as shown in Fig. 5. In addition, it is beneficial for

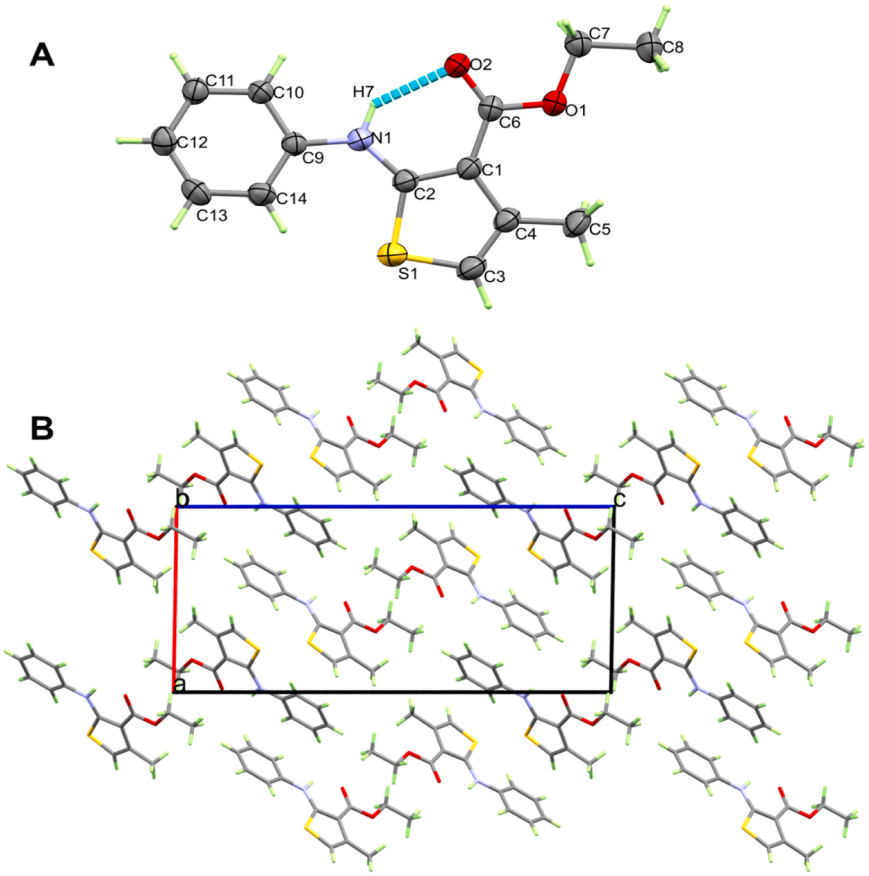

Fig. 2. X-ray structure of **8**. Selected bond distances and angles are depicted in Table 1.

Table 1
Selected X-ray vs DFT-optimized geometrical parameters of **8**.

Distances/Å	X-ray	DFT	Distances/Å	X-ray	DFT
S1-C2	1.716(3)	1.745	O2-C6	1.220(3)	1.230
S1-C3	1.723(4)	1.749	N1-C2	1.360(3)	1.360
O1-C6	1.351(3)	1.350	N1-C9	1.405(3)	1.401
O1-C7	1.451(4)	1.449			
Angles/°	**X-ray**	**DFT**	**Angles/°**	**X-ray**	**DFT**
C2-S1-C3	90.97(15)	91.2	N1-C2-C1	123.6(3)	124.4
C6-O1-C7	115.4(2)	116.4	O2-C6-O1	120.8(3)	121.1
C2-N1-C9	131.6(3)	132.3	O2-C6-C1	125.7(3)	124.5
N1-C2-S1	125.0(2)	124.6			

identifying chemically reactive regions within the molecule, including sites involved in electrophilic and nucleophilic interactions, as well as areas of intra- and intermolecular forces in particular the molecule's potential for hydrogen bonding interactions using the electronic density and charge distribution within the molecule [40]. The color gradient from red to blue in the MEP map indicates the difference in the electrostatic potential. In thiophene **8**, the most electronegative region is observed near the ester carbonyl group oxygen atom (**O17**), represented in deep red on the MEP surface. **O17** carries the maximum negative potential value of 3.866e −2. Therefore, it is the most preferred target for nucleophilic attack. Areas with yellow color, such as the sulfur atom (**S5**) within the thiophene ring and portions of the aromatic system, represent regions of relatively lower negative potential. On the other hand, areas with electropositive groups appear in light blue and are mainly located around the hydrogen atoms attached to the aliphatic side chains. These regions, with a peak potential of +3.866e−2, suggest possible sites for electrophilic attack.

3.6. Frontier molecular orbital (FMO)

The electronic behavior, chemical reactivity, and overall stability of a molecule can be assessed using the frontier molecular orbitals, specifically the highest occupied (HOMO) and the lowest unoccupied (LUMO) molecular orbitals. The HOMO indicates the molecule's ability to donate electrons, whereas the LUMO reflects its affinity to accept electrons. Thus, the energy difference (energy gap) between these orbitals ($\Delta E = E_{LUMO} - E_{HOMO}$) provides insights into the molecule's kinetic stability and chemical hardness.

For thiophene **8**, the calculated HOMO and LUMO energy levels are −5.351 eV and −1.785 eV, respectively, resulting in an energy gap (ΔE) of 3.566 eV. This relatively large HOMO–LUMO gap suggests a high degree of molecular stability and low chemical reactivity, supporting the classification of this compound as a "hard" molecule. The ionization potential (IP) and electron affinity (Ea) are approximated by the negative values of the HOMO and LUMO energies, respectively. Additional global reactivity descriptors such as hardness, softness, electronegativity, and chemical potential are calculated using the following equations [41].

Hardness: $\eta = \frac{(IP-Ea)}{2}$

Chemical potential: $\mu = -\frac{(IP-Ea)}{2}$

Softness: $S = \frac{1}{\eta}$

Electronegativity: $\chi = \frac{(IP+Ea)}{2}$

Fig. 6 shows the spatial distribution of the HOMO and LUMO, which are primarily localized over the thiophene and aromatic rings, and the amino and ester groups, with the extending of HOMO slightly to include the **H31** and **H32** atoms of the terminal methyl group. The ionization potential (IP) and electron affinity (Ea), calculated using the above-mentioned equations, are found to be 5.351 eV and 1.785 eV,

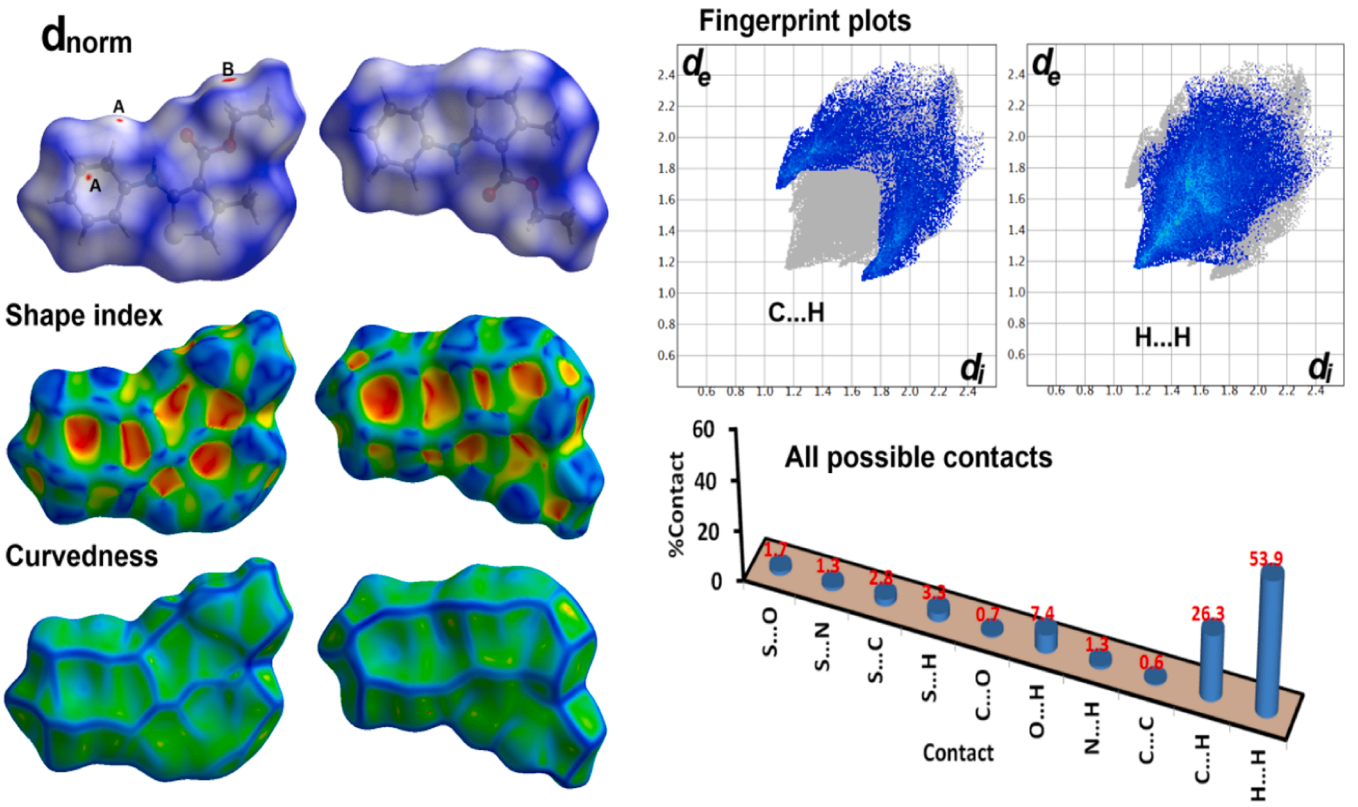

Fig. 3. Hirshfeld analysis of **8**; C…H (A) and C…C (B).

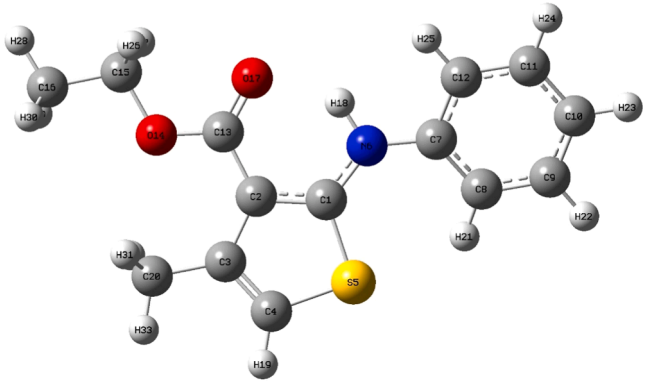

Fig. 4. The optimized structure of thiophene **8**.

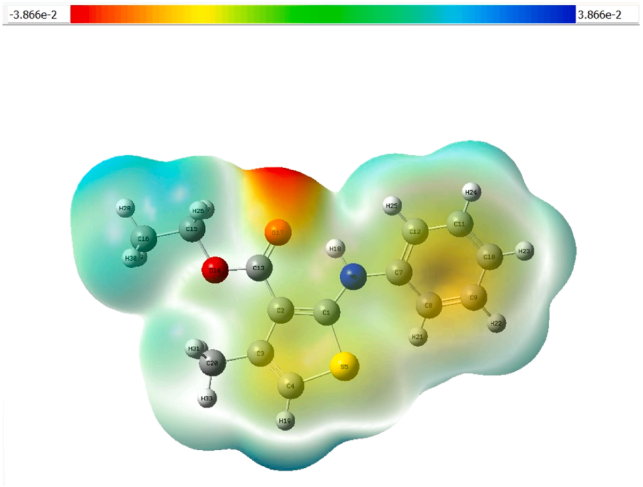

Fig. 5. The MEP map for thiophene **8**.

respectively. In addition, the computed chemical potential (μ), chemical hardness (η), and softness (S) were found −1.783 eV, 1.783 eV, and 0.561 $eV^{-1,}$ respectively. These descriptors indicate that thiophene **8** possesses moderate hardness and electron-accepting ability, consistent with the calculated electronegativity (χ=3.568 eV), indicating a mild tendency to attract electrons.

3.7. Mulliken charge analysis

Mulliken atomic charge distribution plays a key role in quantum chemical analyses, offering insight into the electronic structure, intramolecular interactions, and potential reactive sites within a molecule. Atomic charges influence several physicochemical properties, including dipole moment, polarizability, and charge transfer behavior, making Mulliken analysis an essential tool for understanding donor–acceptor dynamics in molecular systems.

For thiophene **8**, Mulliken atomic charges were computed using DFT/B3LYP methods with 6–311G(d,p) basis sets. The results, shown in **Table S3** and visualized in Fig. 7, reveal that most oxygen and sulfur atoms exhibit negative charges, consistent with their high electronegativity and tendency to attract electron density. Specifically, **O17** and **O14** carry significant negative charges (−0.274 and −0.109, respectively), while **S5** is notably negative at −0.478. Similarly, several carbon atoms, such as **C4, C10, C11, C12**, and **C16,** also carry negative partial charges, suggesting their involvement in π-electron delocalization or electronegative interactions [42].

On the other hand, all hydrogen atoms exhibit positive charges, with the highest observed on **H18** (+0.428) and **H19** (+0.249), indicating their potential role in hydrogen bonding interactions. Some carbon atoms, notably **C1, C8**, and **C15**, show substantial positive charges (e.g.,

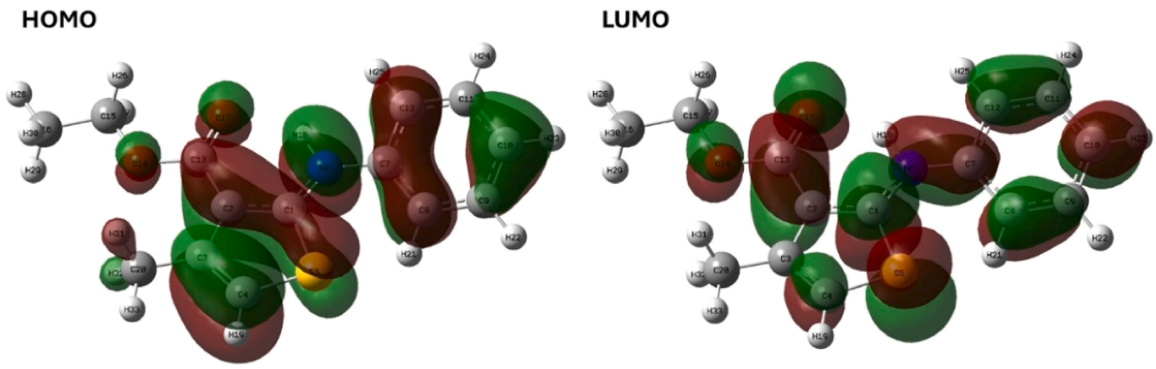

Fig. 6. The HOMO and LUMO levels for thiophene **8**.

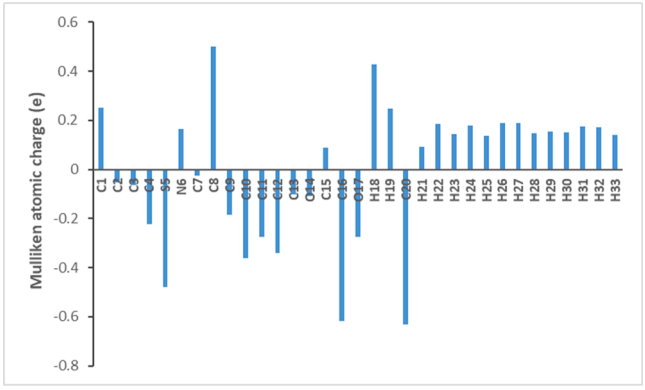

Fig. 7. Plot of Mulliken charge for the thiophene **8** molecule.

C8 = +0.501), which may correspond to electron-deficient centers within the molecular framework. In addition, **N6** appears slightly positive (+0.166), which could reflect its bonding context or resonance effects within the thiophene ring system. These results not only provide a detailed map of charge polarization within thiophene **8** but also help compare its reactivity and electronic behavior with structurally related derivatives. Variations in atomic charges due to substitutions or functional group changes can directly influence molecular interactions and stability.

3.8. *Antitumor evaluation*

Many thiophene derivatives show significant anticancer activity against various cancer cell lines (Fig. 8) [43–45]. In view of these results, the antitumor efficacy of **8** was assessed using the Sulforhodamine B (SRB) assay [32] against HepG2, MCF-7, and HCT116 cell lines. As presented in Table 2, compound **8** showed promising cytotoxicity activity against HepG2 and MCF-7 cell lines. The results of Table 4 and Fig. 8 indicate that the thiophene moiety is a key structural feature responsible for the anticancer activity of various compounds.

Table 2
The cytotoxic effects of **8** on MCF-7, HepG2, and HCT-116 cancer cells.

Compound	IC_{50} (μg/mL)		
	MCF-7	HepG2	HCT-116
8	76.3 ± 2.5	40.1 ± 1.3	92.9 ± 2.02
Doxorubicin	0.92 ± 0.091	0.62 ± 0.04	1.2 ± 0.12

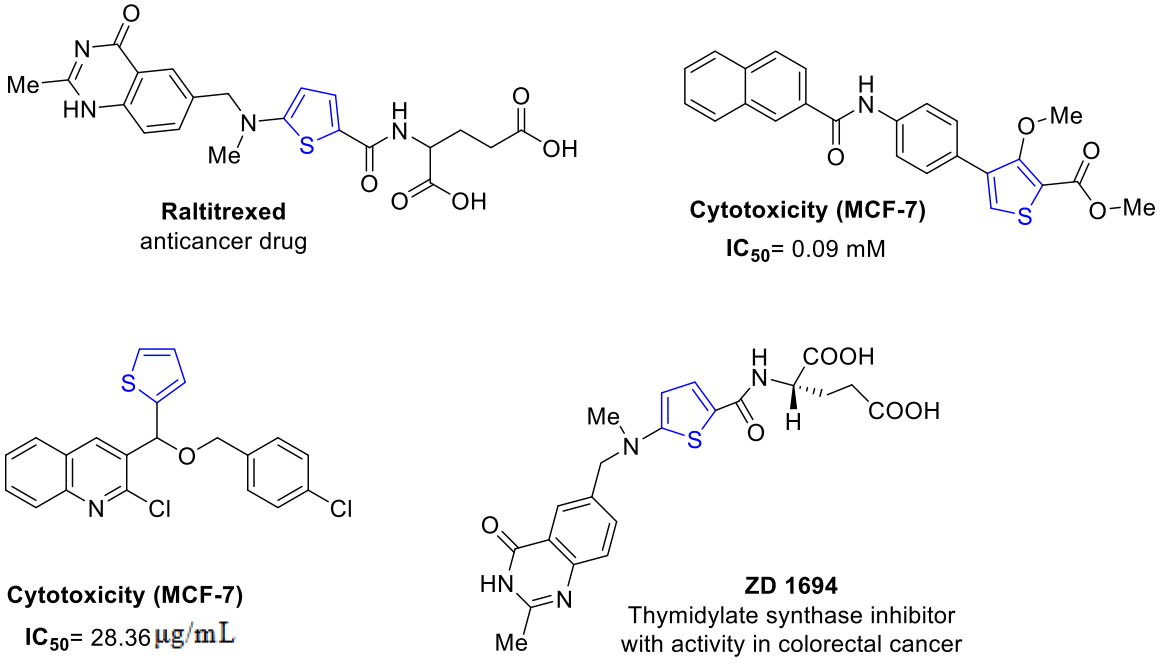

Fig. 8. Anticancer compounds containing thiophene moiety.

3.9. Drug likeness and molecular property prediction

Physicochemical and toxicity parameters of thiophene **8** were predicted using the OSIRIS Property Explorer platform. The OSIRIS interface generates values that are color-coded according to their conformity with drug-like behavior as green indicates favorable (drug-adherent) properties, whereas red highlights parameters that may pose a risk or reduce drug-likeness [33].

Table 3 shows the pharmaceutical attributes of thiophene **8**. The predicted lipophilicity (cLogP) was 3.83 (green), below the threshold value of 5.0 that is often associated with poor absorption, suggesting a high likelihood of adequate permeability across biological membranes. The aqueous solubility value (log $S = -4.03$, green) lies within the range considered acceptable for oral drug candidates (−4.0 to 0.5), indicating solubility sufficient for potential gastrointestinal absorption. The molecular weight (261 Da) and topological polar surface area (TPSA = 66.57 Å^2) were both in the optimal ranges for oral bioavailability (<500 Da and <140 Å^2, respectively), meeting the physicochemical criteria associated with good permeability and transport.

Toxicity-risk predictions showed no alerts for mutagenicity, tumorigenicity, irritancy, or reproductive toxicity, with all parameters displayed in green. This absence of predicted structural toxicophores indicates that, at least *in silico*, the scaffold is unlikely to present intrinsic toxicity liabilities.

Despite these favorable parameters, the drug-likeness score (–3.29, red) suggested that the molecular fragment composition of this compound from those most frequently found in marketed drugs. This score reflects the statistical likelihood that a compound will display drug-like activity based on fragment occurrence in approved pharmaceuticals. The drug-score value of 0.38 (yellow) integrates cLogP, log S, molecular weight, toxicity alerts, and drug-likeness into a single index. While this score indicates moderate overall suitability, it also points to potential for optimization.

Thiophene-containing scaffolds are recognized as privileged structures in medicinal chemistry, with documented activity across antimicrobial, antiviral, anticancer, and anti-inflammatory applications [46, 47]. In particular, N-aryl-substituted thiophenes, such as in thiophene 8, have been linked to enhanced biological activity in antibacterial and anticancer models [48]. Nevertheless, structural modification to improve drug-likeness such as altering substituents on the phenylamino moiety or modifying the ester group may be warranted to enhance pharmacological potential while retaining favorable absorption and toxicity profiles.

Table 3
Physicochemical properties and predicted toxicity risks of thiophene **8** as generated by the OSIRIS Property Explorer interface.

Analysis	Results
Mutagenicity	
Tumorigenicity	
Irritancy	
Reproductive effectiveness	
Molecular Weight (MW)	261
Lipophilicity (cLogP)	3.83
Aqueous solubility	−4.03
Topological polar surface area (TPSA)	66.57
Drug likeness	−3.29
Drug-Score	0.38

4. Conclusion

The synthesis of thiophene derivative **8** has been achieved in excellent yield using a one-pot three-component reaction of ethyl 3-oxobutanoate, phenyl isothiocyanate, and 1-chloropropan-2-one in sodium ethoxide. This method has more advantages such as high yield, short reaction time, easy work-up, and the availability of the starting substrates. Spectroscopic characterizations and single-crystal X-ray diffraction established the structure and the 3D geometry. Hirshfeld analysis indicated the supramolecular packing, and the combined electronic-structure calculations explained the observed interaction patterns. In vitro assays confirmed biological relevance, and in silico screening indicated an acceptable baseline safety profile.

- Single-crystal data and Hirshfeld revealed that the carbonyl group and the adjacent NH are included in a strong N—H…O hydrogen bond, stabilizing the molecular structure of **8**. It is found that the C11…H2 (2.760 Å) and C7…C7 (3.314 Å) contacts appeared as red spots in the d_{norm} map and are considered the most significant for molecular packing. The %C…H and %H…H are 26.3 and 53.9, respectively.
- Computational results supported the experimental findings by identifying reactive centers through Fukui functions and MEP analysis. The HOMO-LUMO gap (3.566 eV) indicated moderate stability, while Mulliken charges and global descriptors confirmed the compound's potential for selective electrophilic and nucleophilic interactions.
- The antitumor activity of thiophene **8** is investigated against MCF-7, HepG2, and HCT-116 cell lines. The IC_{50} values are 76.3 ± 2.5, 40.1 ± 1.3, and 92.9 ± 2.02 µg/mL, respectively.
- *In Silico* test revealed no alerts for mutagenicity, tumorigenicity, irritancy, or reproductive toxicity. The physicochemical parameters were within ranges compatible with oral candidates, with cLogP 3.83, logS −4.03, MW 261 Da, TPSA 66.57 Å^2, drug-likeness −3.29, and drug-score 0.38.

These results indicated the promising anticancer potential of the thiophene derivative **8**.

Funding

The authors extend their appreciation to the Deanship of Research and Graduate Studies at King Khalid University for funding this work through a Large Research Project under grant number RGP2/733/46.

Availability of data and materials

All data generated or analyzed during this study are included in this published article and its supplementary information files.

Ethics approval and consent to participate

Not applicable.

Consent for publication

Not applicable.

Competing interests

The authors declare that they have no competing interests.

CRediT authorship contribution statement

Abdullatif Bin Muhsinah: Writing – review & editing, Writing – original draft, Methodology, Funding acquisition, Data curation,

Conceptualization. **Nabila A. Kheder:** Writing – review & editing, Writing – original draft, Methodology, Investigation, Data curation. **Saied M. Soliman:** Writing – review & editing, Writing – original draft, Methodology, Formal analysis. **Ismail A. Elhaty:** Writing – review & editing, Writing – original draft, Methodology, Formal analysis. **Yahia N. Mabkhot:** Writing – review & editing, Writing – original draft, Methodology, Data curation, Conceptualization.

Declaration of competing interest

The authors declare that they have no known competing financial interests or personal relationships that could have appeared to influence the work reported in this paper

Acknowledgement

The authors extend their appreciation to the Deanship of Research and Graduate Studies at King Khalid University for funding this work through a Large Research Project under grant number RGP2/573/45.

Supplementary materials

Supplementary material associated with this article can be found, in the online version, at doi:10.1016/j.molstruc.2025.144424.

Data availability

Data will be made available on request.

References

[1] I. Jarak, M. Kralj, L. Šuman, G. Pavlović, J. Dogan, I. Piantanida, M. Žinić, K. Pavelić, G. Karminski-Zamola, Novel cyano- and N-isopropylamidino-substituted derivatives of benzo[b]thiophene-2-carboxanilides and benzo[b]thieno[2,3-c]quinolones: synthesis, photochemical synthesis, crystal structure determination, and antitumor evaluation. 2, J. Med. Chem. 48 (7) (2005) 2346–2360, https://doi.org/10.1021/jm049541f.

[2] M.E. Khalifa, W.M. Algothami, Gewald synthesis, antitumor profile and molecular modeling of novel 5-acetyl-4-((4-acetylphenyl)amino)-2-aminothiophene-3-carbonitrile scaffolds, J Mol Struct. 1207 (2020) 127784, https://doi.org/10.1016/j.molstruc.2020.127784.

[3] S.P. Archna, P.A. Chawla, Thiophene-based derivatives as anticancer agents: an overview on decade's work, Bioorg. Chem. 101 (2020) 104026, https://doi.org/10.1016/j.bioorg.2020.104026.

[4] A.B. Muhsinah, N.A. Kheder, S.M. Soliman, H.A. Ghabbour, I.A. Elhaty, N.H. Gad, Y.N. Mabkhot, Novel 1,3-oxathiole derivatives: efficient one-pot synthesis, antitumor efficiency, X-ray crystallographic, Hirshfeld surface, and Fukui function analysis, J Mol Struct. 1331 (2025) 141663, https://doi.org/10.1016/j.molstruc.2025.141663.

[5] A. Bin Muhsinah, M.M. Alharbi, N.A. Kheder, S.M. Soliman, H.A. Ghabbour, N. S. Mahmoud, I.A. Elhaty, Y.N. Mabkhot, New thiophene derivatives: chemoselective synthesis, antitumor effectiveness, structural characterization, DFT calculations, Hirshfeld surface, and Fukui function analysis, BMC Chem. 18 (1) (2024) 228, https://doi.org/10.1186/s13065-024-01346-5.

[6] I.C. Ferreira, R.C. Calhelha, L.M. Estevinho, M.J. Queiroz, Screening of antimicrobial activity of diarylamines in the 2,3,5-trimethylbenzo[b]thiophene series: a structure-activity evaluation study, Bioorg. Med. Chem. Lett. 14 (23) (2004) 5831–5833, https://doi.org/10.1016/j.bmcl.2004.09.038.

[7] I.C. Ferreira, M.J. Queiroz, M. Vilas-Boas, L.M. Estevinho, A. Begouin, G. Kirsch, Evaluation of the antioxidant properties of diarylamines in the benzo[b]thiophene series by free radical scavenging activity and reducing power, Bioorg. Med. Chem. Lett. 16 (5) (2006) 1384–1387, https://doi.org/10.1016/j.bmcl.2005.11.035.

[8] K. Lee, C.W. Park, W.H. Jung, H.D. Park, S.H. Lee, K.H. Chung, S.K. Park, O. H. Kwon, M. Kang, D.H. Park, S.K. Lee, E.E. Kim, S.K. Yoon, A. Kim, Efficacious and orally bioavailable thrombin inhibitors based on a 2,5-thienylamidine at the P1 position: discovery of N-carboxymethyl-d-diphenylalanyl-l-prolyl[(5-amidino-2-thienyl)methyl]amide, J. Med. Chem. 46 (17) (2003) 3612–3622, https://doi.org/10.1021/jm030025j.

[9] M.J.N. Khadri, R. Ramu, N.A. Simha, S.A. Khanum, Synthesis, molecular docking, analgesic, anti-inflammatory, and ulcerogenic evaluation of thiophene-pyrazole candidates as COX, 5-LOX, and TNF-α inhibitors, Inflammopharmacology 32 (1) (2024) 693–713, https://doi.org/10.1007/s10787-023-01364-0.

[10] H. Karaca, S. Kazancı, The metal sensing applications of chalcones: the synthesis, characterization and theoretical calculations, J Mol. Struct. 1248 (2022) 131454, https://doi.org/10.1016/j.molstruc.2021.131454.

[11] A.W. Erian, S.M. Sherif, H.M. Gaber, The chemistry of α-haloketones and their utility in heterocyclic synthesis, Molecules 8 (11) (2003) 793–865, https://doi.org/10.3390/81100793.

[12] Y.N. Mabkhot, F. Alatibi, N.N. El-Sayed, S. Al-Showiman, N.A. Kheder, A. Wadood, A. Rauf, S. Bawazeer, T.B. Hadda, Antimicrobial activity of some novel armed thiophene derivatives and Petra/Osiris/molinspiration (POM) analyses, Molecules 21 (2) (2016), https://doi.org/10.3390/molecules21020222.

[13] A.B. Muhsinah, M.M. Alharbi, S.M. Soliman, N.A. Kheder, H.A. Ghabbour, Y. N. Mabkhot, New thiazole derivatives: synthesis, X-ray crystal structure, Hirshfeld surface analysis, and biological evaluations as potential antimicrobial and antitumor agents, J. Mol. Struct. 1309 (2024) 138235, https://doi.org/10.1016/j.molstruc.2024.138235.

[14] Y.N. Mabkhot, S.S. Al-Showiman, A. Barakat, S.M. Soliman, N.A. Kheder, M. M. Alharbi, A. Asayari, A.B. Muhsinah, A. Ullah, S.L. Badshah, Computational studies of 2-(4-oxo-3-phenylthiazolidin-2-ylidene)malononitrile, BMC Chem. 13 (1) (2019) 25, https://doi.org/10.1186/s13065-019-0542-6.

[15] Y.N. Mabkhot, N.A. Kheder, A. Barakat, M.I. Choudhary, S. Yousuf, W. Frey, Synthesis, antimicrobial, anti-cancer and molecular docking of two novel hitherto unreported thiophenes, RSC Adv. 6 (68) (2016) 63724–63729, https://doi.org/10.1039/C6RA09883E.

[16] Y.N. Mabkhot, M.M. Alharbi, S.S. Al-Showiman, S.M. Soliman, N.A. Kheder, W. Frey, A. Asayari, A. Bin Muhsinah, H. Algarni, A novel synthesis, X-ray analysis and computational studies of (Z)-ethyl 2-((Z)-5-((dimethylamino)methylene)- 4-oxo-3-phenylthiazolidin-2-ylidene)acetate as a potential anticancer agent, BMC Chem. 13 (1) (2019) 35, https://doi.org/10.1186/s13065-019-0554-2.

[17] Y.N. Mabkhot, M.M. Alharbi, S.S. Al-Showiman, H.A. Ghabbour, N.A. Kheder, S. M. Soliman, W. Frey, Stereoselective synthesis, X-ray analysis, computational studies and biological evaluation of new thiazole derivatives as potential anticancer agents, Chem. Cent. J. 12 (1) (2018) 56, https://doi.org/10.1186/s13065-018-0420-7.

[18] A.M. Farag, N.A. Kheder, Y.N. Mabkhot, Synthesis and Antimicrobial evaluation of new pyrazole, thiophene, thiazole and 1,3,4-thiadiazole derivatives incorporating pyrimidine ring, Heterocycles 78 (7) (2009) 1787–1798, https://doi.org/10.3987/COM-09-11682.

[19] Y.A.A. Mohammed, A.A. Abbas, A.M. Fahim, M.S. Nafie, K.M. Dawood, N. A. Kheder, One-pot three-component synthesis, structural characterization, computational investigation, and anti-cancer evaluation of some novel benzo[g][1,3,5]oxadiazocine pyridine carboxamide hybrids, J. Mol. Struct. 1347 (2025) 143269, https://doi.org/10.1016/j.molstruc.2025.143269.

[20] N.A. Kheder, A.M. Fahim, N.S. Mahmoud, K.M. Dawood, Unreported Biginelli product with potent antifungal activity: synthesis, DFT insights, and docking simulation analysis, J. Mol. Struc.t 1330 (2025) 141480, https://doi.org/10.1016/j.molstruc.2025.141480.

[21] N.A. Kheder, S. Tasqeeruddin, N.S. Mahmoud, M.A.A. Mahmoud, I.A. Elhaty, One-pot synthesis of new bis(2,4′-bipyridine), bis(pyrrole), and bis(benzo[f]chromene) derivatives: antimicrobial evaluation, molecular docking, DFT, and ADME profiling, J. Mol. Struct. 1350 (2026) 144065, https://doi.org/10.1016/j.molstruc.2025.144065.

[22] H. Schäfer, H. Jablokoff, M. Hentschel, K. Gewald, 2-Arylamino-thiophen-3-carbonsäurederivate, J. für. Praktische. Chemie. 326 (6) (1984) 917–923, https://doi.org/10.1002/prac.19843260609.

[23] G.M. Sheldrick, SHELXT - integrated space-group and crystal-structure determination, Acta Crystallogr. A Found. Adv. 71 (Pt 1) (2015) 3–8, https://doi.org/10.1107/S2053273314026370.

[24] G.M. Sheldrick, A short history of SHELX, Acta Crystallogr., A, Found. Crystallogr. 64 (Pt 1) (2008) 112–122, https://doi.org/10.1107/S0108767307043930.

[25] M.J. Turner, J.J. McKinnon, S.K. Wolff, D.J.S. Grimwood, P. R., D. Jayatilaka, M.A. Spackman, Crystal Explorer 17 University of Western Australia, 2017.

[26] I. Revvity Signals Software, ChemDraw Professional 16.0, Revvity Signals, Waltham, MA, 2016.

[27] G.W.T.M.J. Frisch, H.B. Schlegel, G.E. Scuseria, M.A. Robb, J.R. Cheeseman, G. Scalmani, V. Barone, G.A. Petersson, H. Nakatsuji, X. Li, M. Caricato, A. Marenich, J. Bloino, B.G. Janesko, R. Gomperts, B. Mennucci, H.P. Hratchian, J.V. Ortiz, A.F. Izmaylov, J.L. Sonnenberg, D. Williams-Young, F. Ding, F. Lipparini, F. Egidi, J. Goings, B. Peng, A. Petrone, T. Henderson, D. Ranasinghe, V.G. Zakrzewski, J. Gao, N. Rega, G. Zheng, W. Liang, M. Hada, M. Ehara, K. Toyota, R. Fukuda, J. Hasegawa, M. Ishida, T. Nakajima, Y. Honda, O. Kitao, H. Nakai, T. Vreven, K. Throssell, J.A. Montgomery, Jr., J.E. Peralta, F. Ogliaro, M. Bearpark, J.J. Heyd, E. Brothers, K.N. Kudin, V.N. Staroverov, T. Keith, R. Kobayashi, J. Normand, K. Raghavachari, A. Rendell, J.C. Burant, S.S. Iyengar, J. Tomasi, M. Cossi, J.M. Millam, M. Klene, C. Adamo, R. Cammi, J.W. Ochterski, R.L. Martin, K. Morokuma, O. Farkas, J.B. Foresman, and D.J. Fox, Gaussian 09W, Revision 9.5, Gaussian, Inc., Wallingford CT, 2016.

[28] A.D. Becke, Density-functional thermochemistry. III. The role of exact exchange, J. Chem. Phys. 98 (1993) 5648–5652, https://doi.org/10.1063/1.464913.

[29] A. Reed, L. Curtiss, F. Weinhold, Intermolecular interactions from a natural bond orbital, donor-acceptor viewpoint, Chem. Rev. 88 (1988) 899–926, https://doi.org/10.1021/cr00088a005.

[30] A.O. Zacharias, A. Varghese, K.B. Akshaya, M.S. Savitha, L. George, DFT, spectroscopic studies, NBO, NLO and Fukui functional analysis of 1-(1-(2,4-difluorophenyl)-2-(1H-1,2,4-triazol-1-yl)ethylidene) thiosemicarbazide, J. Mol. Struct. 1158 (2018) 1–13, https://doi.org/10.1016/j.molstruc.2018.01.002.

[31] S. Scheiner, Comparison of various means of evaluating molecular electrostatic potentials for noncovalent interactions, J. Comput. Chem. 39 (9) (2018) 500–510, https://doi.org/10.1002/jcc.25085.

[32] H.F. Alotaibi, E.S. Khafagy, A.S. Abu Lila, H.F. Alotaibe, S.E. Elbehairi, A. S. Alanazi, M.Y. Alfaifi, J.A. Alamoudi, S.S. Alamrani, F.A. Mokhtar, Anticancer potentials of metformin loaded coconut oil nanoemulsion on MCF-7, HepG2 and HCT-116 cell lines, artificial cells, Nanomed., Biotechnol. 51 (1) (2023) 419–427, https://doi.org/10.1080/21691401.2023.2246145.

[33] T. Sander, J. Freyss, M. von Korff, J.R. Reich, C. Rufener, OSIRIS, an entirely in-house developed drug discovery informatics system, J. Chem. Inf. Model. 49 (2) (2009) 232–246, https://doi.org/10.1021/ci800305f.

[34] K. Gewald, Neuere heterocyclische zwischenprodukte für die Azokupplung durch Cyclisierung von Nitrilen, Chimia 34 (3) (1980) 101, https://doi.org/10.2533/chimia.1980.101.

[35] M. Farhat, A. El-Saghier, M. Makhlouf, K. Kreddan, A. Mezoughi, N. Ketene, S-acetals in heterocyclic synthesis: part 1: synthesis of N-phenyl-2-ylidene and 2,5-diylidene-4-thiazolidinone derivatives, J. Sulfur. Chem. - J. Sulfur. Chem. 28 (2007) 563–572, https://doi.org/10.1080/17415990701586823.

[36] A.B. Muhsinah, A. Alsayari, H. Algarni, S.M. Soliman, N.A. Kheder, H.A. Ghabbour, Y.I. Asiri, K. Venkatesan, Y.N. Mabkhot, Synthesis, X-ray analysis and computational studies of two novel thiophene derivatives, J. Sulfur. Chem. 41 (5) (2020) 517–529, https://doi.org/10.1080/17415993.2020.1769096.

[37] M. Adardour, M. Ait Lahcen, I. Hdoufane, M.M. Alanazi, M. Loughzail, H. Bouzidi Mousser, S. Fleutot, M. François, D. Cherqaoui, A. Baouid, Crystal structure, DFT calculation, and Hirshfeld surface analysis of the 1-(Cyclohex-1-en-1-yl)-3-(prop-2-yn-1-yl)-1,3-dihydro-2H-benzimidazol-2-one, Crystals 13 (12) (2023) 1661, https://doi.org/10.3390/cryst13121661.

[38] R.I. Al-Wabli, K.S. Resmi, Y. Sheena Mary, C. Yohannan Panicker, M.I. Attia, A. A. El-Emam, C. Van Alsenoy, Vibrational spectroscopic studies, Fukui functions, HOMO-LUMO, NLO, NBO analysis and molecular docking study of (E)-1-(1,3-benzodioxol-5-yl)-4,4-dimethylpent-1-en-3-one, a potential precursor to bioactive agents, J. Mol. Struct. 1123 (2016) 375–383, https://doi.org/10.1016/j.molstruc.2016.07.044.

[39] J. Sánchez-Márquez, D. Zorrilla, A. Sánchez-Coronilla, D.M. de los Santos, J. Navas, C. Fernández-Lorenzo, R. Alcántara, J. Martín-Calleja, Introducing "UCA-FUKUI" software: reactivity-index calculations, J. Mol. Model. 20 (11) (2014) 2492, https://doi.org/10.1007/s00894-014-2492-1.

[40] S. Uzun, Z. Esen, E. Koç, N.C. Usta, M. Ceylan, Experimental and density functional theory (MEP, FMO, NLO, Fukui functions) and antibacterial activity studies on 2-amino-4- (4-nitrophenyl) -5,6-dihydrobenzo [h] quinoline-3-carbonitrile, J. Mol. Struct. 1178 (2019) 450–457, https://doi.org/10.1016/j.molstruc.2018.10.001.

[41] N.A. Ancın, S.G. Öztaş, Ö. Küçükterzi, N.A. Öztaş, Theoretical investigation of N-trans-cinnamylidene-m-toluidine by DFT method and molecular docking studies, J. Mol. Struct. 1198 (2019) 126868, https://doi.org/10.1016/j.molstruc.2019.07.115.

[42] O. Noureddine, N. Issaoui, S. Gatfaoui, O. Al-Dossary, H. Marouani, Quantum chemical calculations, spectroscopic properties and molecular docking studies of a novel piperazine derivative, J. King Saud Univ. - Sci. 33 (2) (2021) 101283, https://doi.org/10.1016/j.jksus.2020.101283.

[43] K.C. Gulipalli, S. Bodige, P. Ravula, S. Endoori, G.R. Vanaja, G. Suresh Babu, J. N. Narendra Sharath Chandra, N. Seelam, Design, synthesis, in silico and in vitro evaluation of thiophene derivatives: a potent tyrosine phosphatase 1B inhibitor and anticancer activity, Bioorg. Med. Chem. Lett. 27 (15) (2017) 3558–3564, https://doi.org/10.1016/j.bmcl.2017.05.047.

[44] D.I.A. Othman, K.B. Selim, M.A.A. El-Sayed, A.S. Tantawy, Y. Amen, K. Shimizu, T. Okauchi, M. Kitamura, Design, synthesis and anticancer evaluation of new substituted thiophene-quinoline derivatives, Bioorg. Med. Chem. 27 (19) (2019) 115026, https://doi.org/10.1016/j.bmc.2019.07.042.

[45] A.L. Jackman, D.C. Farrugia, W. Gibson, R. Kimbell, K.R. Harrap, T.C. Stephens, M. Azab, F.T. Boyle, ZD1694 (Tomudex): a new thymidylate synthase inhibitor with activity in colorectal cancer, Eur. J. Cancer 31 (7) (1995) 1277–1282, https://doi.org/10.1016/0959-8049(95)00166-G.

[46] A.B. Muhsinah, N.A. Kheder, S.M. Soliman, H.A. Ghabbour, I.A. Elhaty, N. S. Mahmoud, M.A.A. Mahmoud, Y.N. Mabkhot, Chemoselective synthesis, structural elucidation, antitumor activity, Hirshfeld surface, and Fukui functions analysis of new thiophene derivatives, J. Mol. Struct. 1343 (2025) 142826, https://doi.org/10.1016/j.molstruc.2025.142826.

[47] R. Shah, P.K. Verma, Therapeutic importance of synthetic thiophene, Chem. Cent. J. 12 (1) (2018) 137, https://doi.org/10.1186/s13065-018-0511-5.

[48] Y.N. Mabkhot, N.A. Kaal, S. Alterary, S.S. Al-Showiman, T.A. Farghaly, M. S. Mubarak, Antimicrobial activity of thiophene derivatives derived from ethyl (E)-5-(3-(dimethylamino)acryloyl)-4-methyl-2-(phenylamino)thiophene-3-carboxylate, Chem. Cent. J. 11 (1) (2017) 75, https://doi.org/10.1186/s13065-017-0307-z.